ORIGINAL RESEARCH

# Integrin αvβ3 and LHRH Receptor Double Directed Nano-Analogue Effective Against Ovarian Cancer in Mice Model

Na Qi [1],*, Xiantai Zhou[2],*, Ningzhu Ma[2], Jianguo Zhang[2], Zhenlin Wang[2], Xin Zhang[1], Aimin Li [1]

[1]Cancer Center, Integrated Hospital of Traditional Chinese Medicine, Southern Medical University, Guangzhou, 510315, People's Republic of China; [2]Department of Pharmacy, Guilin Medical University, Guilin, 541004, People's Republic of China

*These authors contributed equally to this work

Correspondence: Aimin Li; Xin Zhang, Cancer Center, Integrated Hospital of Traditional Chinese Medicine, Southern Medical University, Guangzhou, 510315, People's Republic of China, Email liaimin2005@163.com; 252089553@qq.com

**Introduction:** The high mortality rate of malignant ovarian cancer is attributed to the absence of effective early diagnosis methods. The LHRH receptor is specifically overexpressed in most ovarian cancers, and the integrin αvβ3 receptor is also overexpressed on the surface of ovarian cancer cells. In this study, we designed LHRH analogues (LHRHa)/RGD co-modified paclitaxel liposomes (LHRHa-RGD-LP-PTX) to target LHRH receptor-positive ovarian cancers more effectively and enhance the anti-ovarian cancer effects.

**Methods:** LHRHa-RGD-LP-PTX liposomes were prepared using the thin film hydration method. The morphology, physicochemical properties, cellular uptake, and cell viability were assessed. Additionally, the cellular uptake mechanism of the modified liposomes was investigated using various endocytic inhibitors. The inhibitory effect of the formulations on tumor spheroids was observed under a microscope. The co-localization with lysosomes was visualized using confocal laser scanning microscopy (CLSM), and the in vivo tumor-targeting ability of the formulations was assessed using the IVIS fluorescent imaging system. Finally, the in vivo anti-tumor efficacy of the formulations was evaluated in the armpits of BALB/c nude mice.

**Results:** The results indicated that LHRHa-RGD-LP-PTX significantly enhanced cellular uptake in A2780 cells, increased cytotoxicity, and hand a more potent inhibitory effect on tumor spheroids of A2780 cells. It also showed enhanced co-localization with endosomes or lysosome in A2780 cells, improved tumor-targeting capability, and demonstrated an enhanced anti-tumor effect in LHRHR-positive ovarian cancers.

**Conclusion:** The designed LHRHa-RGD-LP-PTX liposomes significantly enhanced the tumor-targeting ability and therapeutic efficacy for LHRH receptor-positive ovarian cancers.

**Keywords:** modified liposome, LHRHa, RGD, paclitaxel, ovarian cancer

## Introduction

Ovarian cancer is one of the most lethal gynecological malignancies, difficult to diagnose early, and is characterized by a poor prognosis.[1,2] Currently, the treatment for ovarian cancer mainly involves surgery and platinum/taxane-based chemotherapy; however, the majority of patients experience recurrence months to years after diagnosis.[3,4] Generally, ovarian cancer is hormone-dependent. The expression level of the Luteinizing hormone-releasing hormone (LHRH) receptor is significantly increased in nearly 80% of human ovarian cancer cells, while its expression is minimal in most other healthy organs.[5,6]

Physiologically, LHRH is synthesized in the hypothalamus and secreted from the pituitary.[6] Natural LHRH is unstable and rapidly degraded in vivo; therefore, LHRH analogue (LHRHa) was synthesized for improved stability and bioactivity to target LHRH receptor.[7] Compared to conventional protein macromolecules (LHRH), LHRHa peptides offer several advantages, including lower antigenicity, better stability, and easier preparation. Used as an active targeting

**3071**

**Graphical Abstract**
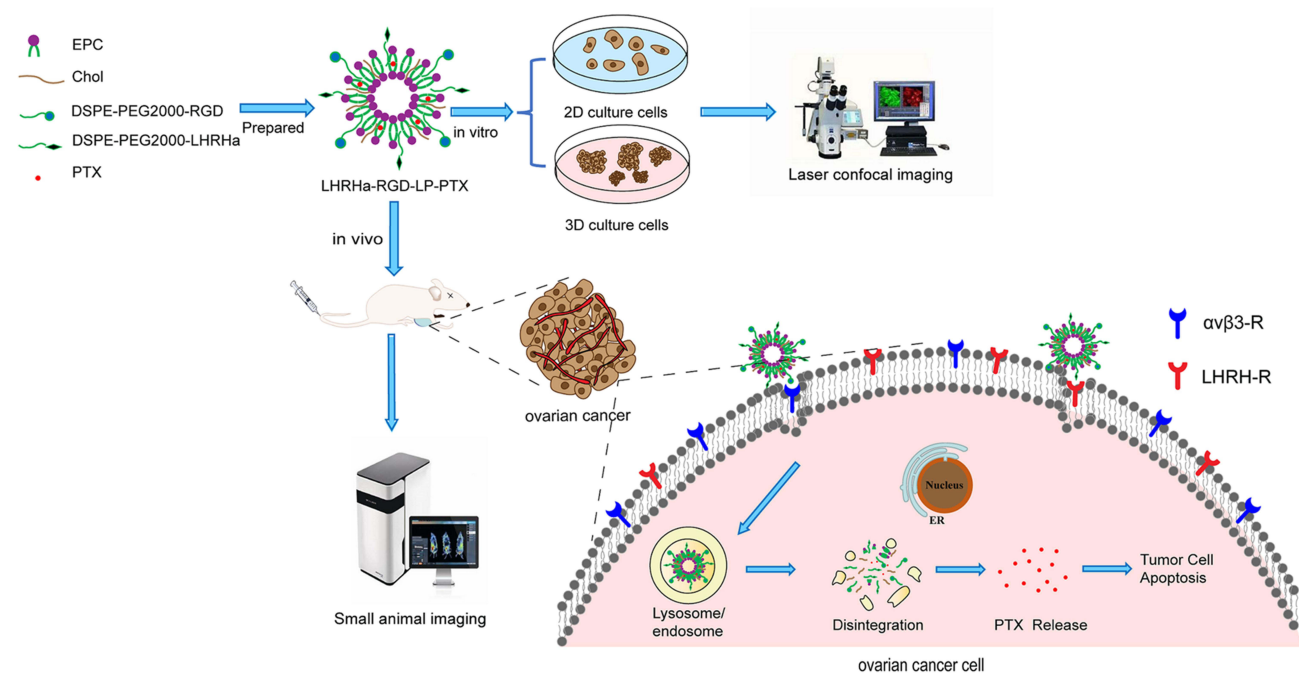


ligand, LHRHa enables specific delivery of diagnostic or therapeutic drugs to LHRH receptor-positive cancer cells.[8,9] This approach significantly improves diagnostic or therapeutic efficacy, while substantially limiting adverse side effects on healthy tissues.[6,10,11] Several studies have suggested that the mechanism of LHRHa-modified drug delivery systems may be related to receptor-mediated endocytosis in LHRH receptor-positive cancer cells.[7,11] Furthermore, it has been reported that LHRHa-modified drug delivery systems show no toxicity to the pituitary and almost no influence on the concentration or reproductive functions of luteinizing hormone.[6] In summary, LHRHa emerges as a promising targeting ligand for targeted drug delivery systems to treat ovarian cancers.

Integrin αvβ3 receptor is overexpressed on the surface of cancer cells, and RGD peptide can specifically bind to integrin αvβ3 receptor. RGD, as a targeting moiety, has been widely used in modified drug delivery systems (TDDS) for both the treatment and imaging of cancer.[12,13] Additionally, we previously reported that RGD-modified liposomes significantly enhanced the penetration effect into tumor spheroids, and we found that RGD modification had a dominant effect on promoting tumor spheroids penetration.[14]

Paclitaxel (PTX), one of the taxane antineoplastic agents, is a first-line chemotherapy agent for treating ovarian cancer. However, several severe adverse side effects of PTX remain problematic in clinical use, including induced hypersensitivity reactions, myelosuppression, neurotoxicity, and cardiotoxicity.[15] Liposomes have been used as a chemotherapy drug carrier to decrease its adverse effects. Some studies have demonstrated the advantages of using liposomes in the treatment of ovarian cancer.[16]

In this study, we designed LHRHa/RGD co-modified paclitaxel liposomes to improve the targeting of ovarian cancer and enhance the anti-ovarian cancer effect. LHRHa and RGD specifically bind to the LHRH receptor and integrin αvβ3 receptor on the surface of ovarian cancer cells, respectively. We utilized these characteristics to enhance the targeting effect on ovarian cancer. Furthermore, we used RGD modification to facilitate liposome penetration into deep tumor tissue. The modified liposomes were evaluated and characterized in vitro. To compare the influence of LHRH receptor on the surface of ovarian cancer cells, cell experiments in vitro were conducted using LHRH receptor-positive A2780 and LHRH receptor-negative SKOV3 ovarian cancer cells to investigate cytotoxicity, cellular uptake, uptake mechanisms,

tumor spherical inhibition effect, and lysosome co-localization of the targeting delivery system. The targeting characteristics of the LHRHa and RGD modified targeting delivery system were evaluated by in vivo imaging, and the anti-tumor effects of the LHRHa and RGD modified targeting delivery system were tested in vivo in a subcutaneous A2780 ovarian cancer xenograft model.

# Materials and Methods

## Materials

Egg distearoylphosphatidylcholine (EPC) was sourced from Lipoid GMBH (Germany). DSPE-PEG$_{2000}$ and DSPE-PEG$_{2000}$-RGD were purchased from Shanghai Ponsure Biotech, Inc. (Shanghai, China). Cholesterol (Chol) was provided by Shanghai Xingzhi Chemical Factory (Shanghai, China). PTX was obtained from Wuhan bio-cata Biological Technology Co., Ltd (Wuhan, China). Coumarin-6 (C6, purity > 98%) was purchased from Sigma Aldrich (St. Louis, USA). 1,1'-dioctadecyl-3, 3, 3', 3'-tetramethylindotricarbocyanine iodide (DiR) dye was obtained from Yeasen Biotechnology (Shanghai, China). DMEM medium was supplied by Gibco (CA, USA). Fetal bovine serum (FBS) was sourced from GEMINI (USA). The high-performance liquid chromatography (HPLC)-grade solvents used for HPLC were obtained from Xiqiao Chemical Co., Ltd. (Shantou, China). Other chemicals and reagents were obtained commercially and were of analytical grade. Ultrafiltration centrifugal tube (molecular weight cut-off: 10,000) were supplied from Millipore (Massachusetts, USA). DSPE-PEG$_{2000}$-LHRHa (LHRHa peptides with amino acid sequence:[17] His-Trp-Ser-Tyr-D-Leu-Leu-Arg-Pro-Gly-Cys) were synthesized by ChinaPeptides Co., Ltd (Shanghai, China), with the Time-of-Flight Mass Spectrometry results shown in Figure S1).

## Animals and Cell Culture

The human ovarian cancer cell lines A2780 (LHRH receptor positive) and SKOV3 (LHRH receptor-negative) were obtained from Shanghai Guandao Biological Engineering Co., Ltd (Shanghai, China). Ovarian cancer cells were cultured in DMEM medium supplemented with 10% fetal bovine serum (FBS) and 1% antibiotics (penicillin and streptomycin). The cells were maintained in a 37°C incubator with 5% CO$_2$. Male BALB/c nude mice (5–6 weeks, 18–20 g) were purchased from Hunan Silaike Laboratory Animal Co, Ltd (Hunan, China). All nude mice were housed in a SPF animal room at 25°C, with relative humidity maintained at 40% - 70%. All animal experiments were conducted with approval from the Guilin Medical University Institutional Animal Care and Use Committee (The Tab of Animal Experimental Ethical Inspection, No.2020–0004). All animal experiments were performed in accordance with the "Guidance for the Care and Use of Laboratory Animals".

## Preparation of Modified Liposomes

Epc, Chol, DSPE-PEG$_{2000}$, RGD-DSPE-PEG$_{2000}$, LHRHa-DSPE-PEG$_{2000}$, PTX were combined in a molar ratio (95:20:5:0.1:0.1:5). The lipid and drug mixture were dissolved in a chloroform and methanol solution (3:1, v:v). Modified Liposomes were prepared using the thin film hydration method as previously described.[14] Subsequently, free PTX was removed from the liposomes using an equilibrium dialysis method.

## Characterization of Liposomes Size, Zeta Potential, and EE

The particle size and zeta potential of the modified liposomes were measured using a Zetasizer Nano ZS (Malvern Instruments, Worcestershire, UK). Each sample was analyzed in triplicate. The morphology of the modified liposomes was examined using a transmission electron microscope (TEM) (HITACHI Limited, Japan). The sample was dropped onto a carbon film coated copper TEM grid, air-dried, then the grid was immersed in a drop of 1% phosphotungstic acid staining for 2 min, and air-dried 1 h at room temperature. The encapsulation efficiency (EE) of liposomes was determined by the dialysis method. Liposomes were dialyzed using a dialysis tube (MWCO, 8000–12,000 Da) for 8 h, and the dialysate was analyzed using a HPLC (SHIMADZU Corporation, Japan), with a Hypersil BDS C18 column (250 mm×4.6 mm, 5μm, Thermo Fisher Scientific Technologies Inc., USA). The mobile phase consisted of

acetonitrile/water (50/50; v/v) at a flow rate of 1.0 mL/min. The wavelength was set at 228 nm and the column temperature was maintained at 28°C. All experiments were conducted in triplicate.

## In vitro Drug Release Assays

The in vitro release of liposomes was assessed using the dialysis method. A 2 mL sample was placed in a dialysis tube (MWCO, 8000–12,000 Da), sealed, then submersed in 30 mL of pH 7.4 PBS (0.01M) containing sodium salicylate (1 mol·L$^{-1}$), with stirring at 100 rpm at 37°C. In vitro release was monitored from 1 to 72 h at predetermined time points. For each measurement, the dialysate outside the dialysis tube was collected and analyzed by HPLC as previously described.[18] The in vitro cumulative release curve was then plotted. The stability of liposomes in vitro were assessed in 50% fetal bovine serum (FBS) at predetermined time points (1,2, 4, 8, 12 and 24 h) as described previously.[14,18] A 28-day stability of liposomes at 4°C was investigated by measuring the liposome particle size and polydispersity index (PDI).

## In vitro Cytotoxicity Assay of Formulations

The cytotoxicity of free PTX and the various liposomal formulations against SKOV3 and A2780 cells was evaluated using the MTT assay.[18] Cells were seeded in 96-well microplates at a density of $1 \times 10^4$ cells/well and incubated for 24 h. The culture media were then replaced with either free PTX or PTX liposomal formulations with serial concentrations. After 48 h of exposure, 20 μL of 5 mg/mL MTT solution was added to the wells, and the plates were incubated for 4 h in the dark. Subsequently, the media were removed, and 150 μL of DMSO was added to each well to dissolve the purple formazan crystals. The absorbance at 492 nm was measured using a Microplate reader (Bio-Tek, USA). Cell viability was calculated using the following formula.[14]

$$\text{Cell viability}(\%) = \left(A_{\text{sample}} / A_{\text{control}}\right) \times 100\%$$

## Cellular Uptake of Modified Liposomes

To study cellular uptake, SKOV3 and A2780 cells were seeded on glass coverslips in 12-well plates ($5 \times 10^4$ cells/well). After 24 h of growth, the cells were treated with 5 μg/mL C6-loaded liposomes and incubated for 4 h at 37°C. Then, the cells were washed thrice with PBS for 5 min each, fixed with 4% (wt/vol) paraformaldehyde, and the nuclei were stained with 5 μg/mL Hochest -33342 for 10 min. Cellular uptake of liposomes was observed using a fluorescence microscope (DM500, Zeiss, Germany) for semi-qualitative analysis. For quantitative analysis, 500μL of DMSO was added to each well, then 150 μL of the sample was collected, and the fluorescence intensity was measured at 466/505 nm (Ex = 466 nm, Em = 504 nm) using a fluorescent plate reader (Bio-Tek, USA).

## The Study of Uptake Mechanisms Using Endocytosis Inhibitors

SKOV3 and A2780 cells were seeded in 96-well plates at a density of $1 \times 10^4$ cells per well and cultured overnight. After 24 h, the cells were pre-incubated with various endocytosis inhibitors at 37 °C for 30 min,[15] including filipin (5 μg/mL), amiloride (15 μg/mL), cytochalasin D (2 μg/mL), chlorpromazine (10 μg/mL), LHRHa (200 μg/mL), RGD (200μg/mL), LHRHa + RGD (200 μg/mL for each moiety). Then, the medium was replaced with fresh medium containing LHRHa-RGD-LP-C6, and the cells were further incubated for 4 h at 37 °C. Afterwards, the cells were rinsed three times with PBS, and 1% TritonX-100 was added and incubated for 40 min in the dark. The fluorescence intensity was measured at 466/505 nm (Ex = 466 nm, Em = 504 nm) using a fluorescent microplate (Bio-Tek, USA).

$$\text{Relative uptake rate} = \left(A_{\text{negative}} - A_{\text{blank}}\right) / \left(A_{\text{positive}} - A_{\text{blank}}\right) \times 100\%$$

## The Inhibitory Effect on Tumor Spheroids

SKOV3 and A2780 three-dimensional tumor spheroids were cultured as previously described.[18] The bottom of a 96-well plate was pre-coated with 2% low melting point agarose and heated at 37°C for 2h. Then, $1 \times 10^3$ cells/well were seeded in 96-well microplate, shaken for 10 min (1500 rpm/min), and incubated at 37°C with 5% $CO_2$. Upon reaching 200 μm in diameter, the tumor spheroids were treated with PTX liposomes and incubated for 48 h. The culture medium containing PTX liposomes was refreshed every 2 days, and the longest diameter of the tumor spheroids was measured every 2 days. The relative longest diameter of tumor spheroids (%) was compared with that of day 0.

## Confocal Imaging Analysis on Endocytosis Pathways

SKOV3 or A2780 cells were seeded in glass-bottom cell culture dishes at a density of $1 \times 10^5$ per well. After 24 h of cell culture, the cells were incubated with 2 μg/mL LHRHa-RGD-LP-C6 liposomes for 2 h at 37 °C. The cells were then washed three times with PBS, and 1 mL of 75 nM lysotracker was added to the cell culture media for 1 h. After rinsing three times with PBS, 500μL of 5 μg/mL Hochest 33342 was added for 15 min. The cells were fixed for 20 min in 4% paraformaldehyde, sealed with anti-quenchant, and examined under confocal microscopy in Z-stack mode.

## In vivo Fluorescent Imaging

The A2780 armpit tumor model was established by transplanting A2780 cells ($5 \times 10^6$ cells/100 μL) into the armpit of BALB/c mice. When the tumor volume reached approximately 100 $mm^3$, 200 μL of DiR-labelled liposomes (1 mg/kg) were injected into the lateral tail vein of BALB/c nude mice bearing tumors. Post-injection, the mice were anesthetized with isoflurane and underwent fluorescence imaging at 4, 8, 12, and 24 h using the IVIS (PerkinElmer, Lumina III, USA). At 24 h post-injection, the mice were euthanized using ether, and major organs, including the heart, lungs, spleen, liver, kidneys, and tumors were collected for further fluorescent imaging (Ex=740 nm/Em=790 nm) using the IVIS.[18]

## Evaluation of in vivo Anti-Tumor Efficacy

Initially, $5 \times 10^6$ A2780 cells (100 μL) were implanted into the armpit of BALB/c nude mice. Treatment commenced when the tumor volume reached approximately 50~100 $mm^3$. Animals were randomized divided into 5 groups (n=5): PBS, PEG-LP-PTX, RGD-LP-PTX, LHRHa-LP-PTX, and LHRHa-RGD-LP-PTX. These formulations were administered into the tail vein of nude mice bearing tumors at a PTX dose of 5 mg/kg body weight. Administration was carried out once every 2 days for a continuous period of 14 days. Body weights and tumor volumes were monitored every 2 days. The tumor volume was calculated using the formula: tumor volume ($mm^3$) $=0.5 \times (length \times width^2)$.[19] At the end of the treatment, all nude mice were euthanized by cervical dislocation under ether anesthesia, and the tumors were collected and weighed. The tumor, heart, liver, spleen, lung and kidney were harvested, fixed, and stained with hematoxylin-eosin (HE). The TUNEL assay of the tumors was conducted according to the manufacturer's protocol.

## Statistical Analysis

Five mice in each group were used for the in vivo anti-tumor study, and three mice in each group were used for the in vivo imaging study. Data were analyzed using GraphPad Prism 8 software. Student's t-test was employed to evaluate differences between two groups, while one-way ANOVA was used to assess differences among three or more groups. Differences were considered statistically significant at $p < 0.05$ (*), and very significant at $p < 0.01$ (**).

# Results and Discussion

## Characterization of Liposomes

In this study, we prepared stable liposomes conjugated with LHRHa and RGD (LHRHa-RGD-LP-PTX). The mean particle size of LHRHa-RGD-LP-PTX was 108.52±1.63 nm with a polydispersity index (PDI) of 0.23±0.022, indicating

a narrow size distribution. The mean particle size of LHRHa-RGD-LP-PTX was approximately 15–20 nm larger than that of PEG-LP-PTX. Similarly, the particle size of RGD-PEG-PTX showed a modest increase compared to PEG-LP-PTX, attributable to the coupling of LHRHa or RGD small peptides to the liposome surface. This observation is consistent with previous reports.[11] The zeta potential of PEG-LP-PTX was −31.17±0.15 mV, explained by the inclusion of negatively charged DSPE-PEG$_{2000}$ in the liposome membrane.[20] The zeta potential of LHRHa-RGD-PEG-PTX was −22.07±1.56 mV. This slight decrease, compared to PEG-LP-PTX, is due to weak positive charge of the RGD and LHRHa peptides linked to the liposomal membrane.[21] Considering that a 100 nm size liposome contains approximately 100,000 molecules of phospholipids,[22] we estimated that around 108 RGD molecules and 108 LHRHa molecules are conjugated per liposome. As shown in Table 1, the EE of PEG-LP-PTX, RGD-LP-PTX, LHRHa-LP-PTX, LHRHa-RGD-LP-PTX were 83.95±5.16%, 80.51±4.00%, 91.75±5.28%, and 84.74±3.14%, respectively. The EE of RGD-LP-PTX slightly decreased compared to PEG-LP-PTX, possibly due to RGD's role as a cell-penetrating peptide enhancing liposome membrane permeability.[14] However, the EE of LHRHa-LP-PTX increased, potentially due to the hydrophobic interactions among LHRHa, PC (lipid), and PTX, which may reduce PTX leakage from liposomes. Consequently, the drug loading content (DLC) of LHRHa-LP-PTX was also higher (Table 1). The EE of LHRHa-RGD-LP-PTX remained almost unchanged compared to PEG-LP-PTX, a result of the combined modification by RGD and LHRHa. The morphology of PEG-LP-PTX, RGD-LP-PTX, LHRHa-LP-PTX and LHRHa-RGD-LP-PTX, observed via transmission electron microscopy (TEM) and presented in Figure 1A, shows an average diameter of 100–150 nm with no particle aggregation, aligning with the dynamic laser scattering measurements.

The in vitro release of PTX from the liposomes indicated that PTX was released into the medium with a rapid release rate of 86.5% at 72 h, as shown in Figure 1B. In comparison, the release profiles of PEG-LP-PTX demonstrated a sustained PTX release, with a cumulative release of 37.2% at 72 h. This difference is attributed to the PEGylated hydrophilic bonds on PEG-LP-PTX's surface hindering PTX release, as previously reported.[14,23] Conversely, RGD-LP-PTX exhibited faster PTX release properties than PEG-LP-PTX, potentially due to RGD enhancing the bilayer membrane permeability of the liposomes. LHRHa-RGD-LP-PTX and LHRHa-LP-PTX showed similar in vitro cumulative release profiles compared to PEG-LP-PTX. We hypothesize that the LHRHa peptide coating on the liposome surface and its hydrophobic interactions with PC (lipid) and PTX further slow PTX release. The average particle size and PDI of all tested liposomes changed by less than 10% over 24 h in 50% fetal bovine serum (FBS) at 37 °C, as demonstrated in Figures 1C and D, suggesting that the liposomes were relatively stable with no significant aggregation. Additionally, Figure 1E and F demonstrated that the particle size and PDI of the liposomes in each group exhibited no significant variation at 4°C over a 28-day period. We deduce that all measured liposomes were stable at 4 °C for 28 days.

## Cytotoxicity Assay

The in vitro cytotoxicity of free PTX and PTX-loaded liposomes on LHRH receptor-negative SKOV3 cells and LHRH receptor-positive A2780/DDP cells was investigated using an MTT assay. After incubating with SKOV3 cells for 48 h, the IC50 values of PTX, PEG-LP-DTX, RGD-LP-PTX, LHRHa-LP-PTX, and LHRHa-RGD-LP-PTX were 0.57, 0.45, 0.24, 0.36 and 0.19 μg/mL, respectively. As depicted in Figure 2A, RGD-LP-PTX demonstrated stronger cytotoxicity than PEG-LP-PTX (p<0.05), and LHRHa-RGD-LP-PTX exhibited higher cytotoxicity than LHRHa-LP-PTX (p<0.05). However, LHRHa-LP-PTX did not show significant higher cytotoxicity than PEG-LP-PTX (p>0.05), and similarly, LHRHa-RGD-LP-PTX did not exhibit higher cytotoxicity than RGD-LP-PTX (p>0.05). Cytotoxicity is generally

**Table 1** Characterization of Paclitaxel-Loaded Liposomes (n=3)

| Group | Particle Size (nm) | Zeta Potential (mV) | PDI | EE(%) | DLC(%) |
|---|---|---|---|---|---|
| PEG-LP-PTX | 91.08±1.08 | −31.17±0.15 | 0.22±0.027 | 83.95±5.16% | 3.44±0.50% |
| RGD-LP-PTX | 95.96±2.05 | −29.40±0.87 | 0.24±0.003 | 80.51±4.00% | 3.57±0.22% |
| LHRHa-LP-PTX | 106.92±3.08 | −27.37±1.45 | 0.24±0.010 | 91.75±5.28% | 3.89±0.39% |
| LHRHa-RGD-LP-PTX | 108.52±2.63 | −22.07±1.56 | 0.23±0.022 | 84.74±3.14% | 3.54±0.09% |
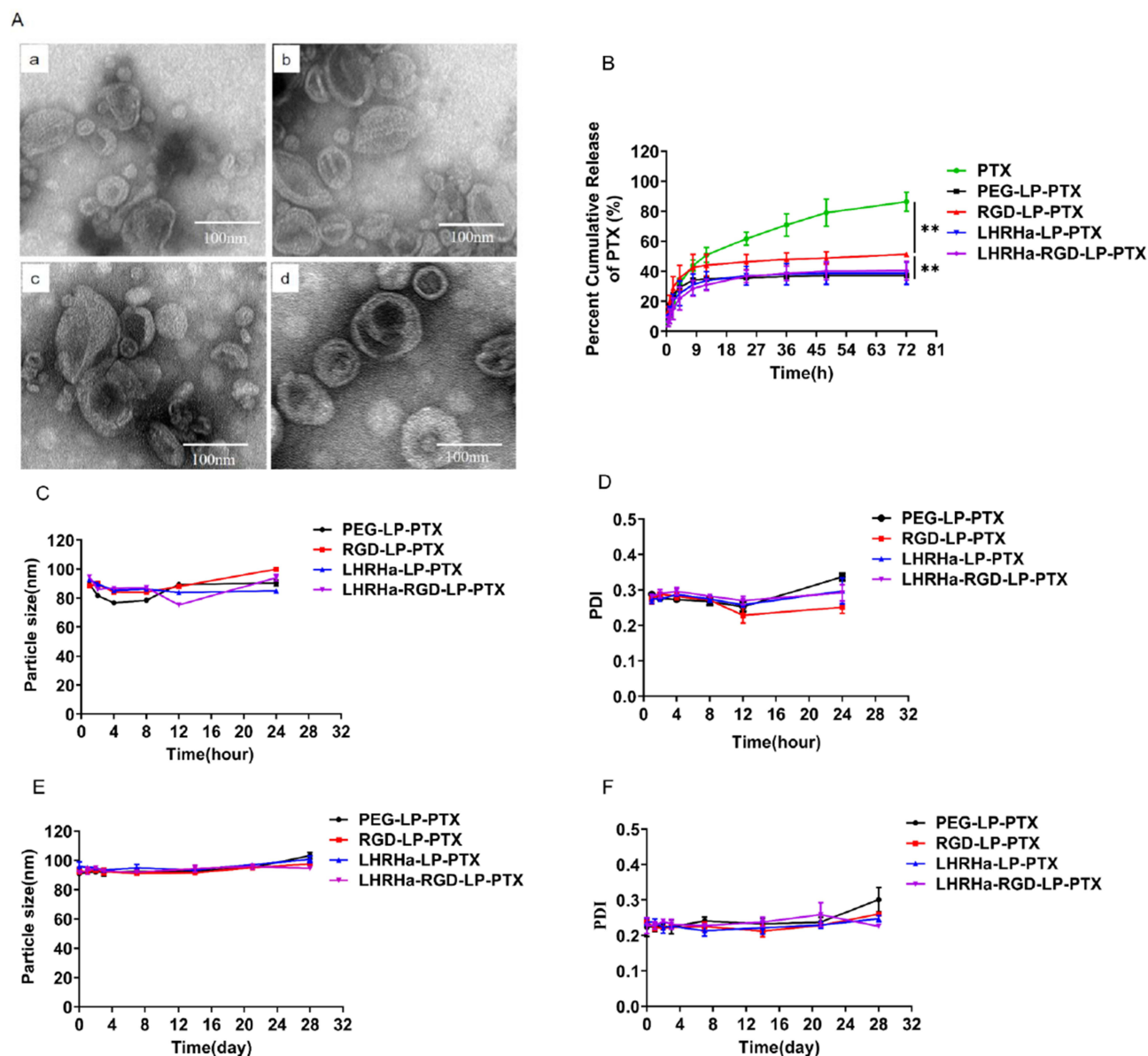
**Figure 1** (**A**) Transmission electron micrograph (TEM) of PEG-LP-PTX(a), RGD-LP-PTX(b), LHRHa-LP-PTX(c) and LHRHa-RGD-LP-PTX(d). (**B**) In vitro release of PTX-loaded liposomes and PTX. Data represented the mean ± SD (n =3), **$p < 0.01$. (**C**) Observation of variations in average particle size of liposomes in 50% FBS at 37 °C. (**D**) Observation of variations in PDI of liposomes in 50% FBS at 37 °C. (**E**) Observation of variations in average particle size at 4 °C over 28 days. (**F**) Observation of variations in PDI of liposomes 4 °C over 28 days. Data represent the mean ± SD (n =3).

correlated with the results of cellular uptake. For the LHRHa-RGD-LP-PTX and RGD-LP-PTX groups, we speculate that RGD modification plays a major role in increasing cellular uptake and enhancing cytotoxicity in LHRH receptor-negative SKOV3 cells.

After incubation with A2780 cells for 48 h, the calculated IC50 values from the cytotoxicity results were 0.43, 0.32, 0.19, 0.18, and 0.10 μg/ mL for PTX, PEG-LP-DTX, RGD-LP-PTX, LHRHa-LP-PTX, and LHRHa-RGD-LP-PTX, respectively. From Figure 2B, the in vitro cytotoxicity of free PTX and PTX-loaded liposomes on A2780 cells exhibited concentration-dependent effects. The results showed that PTX-loaded liposomes had a higher inhibitory effect of tumor cells compared to free PTX, which might be related to nanosized liposomes enhancing cell uptake in tumor cells.[23,24] Both LHRHa-LP-PTX and RGD-LP-PTX demonstrated higher cytotoxicity on A2780 cells than PEG-LP-PTX. This indicated that RGD or LHRHa modification enhanced the inhibitory effect on tumor cells, possibly due to enhanced
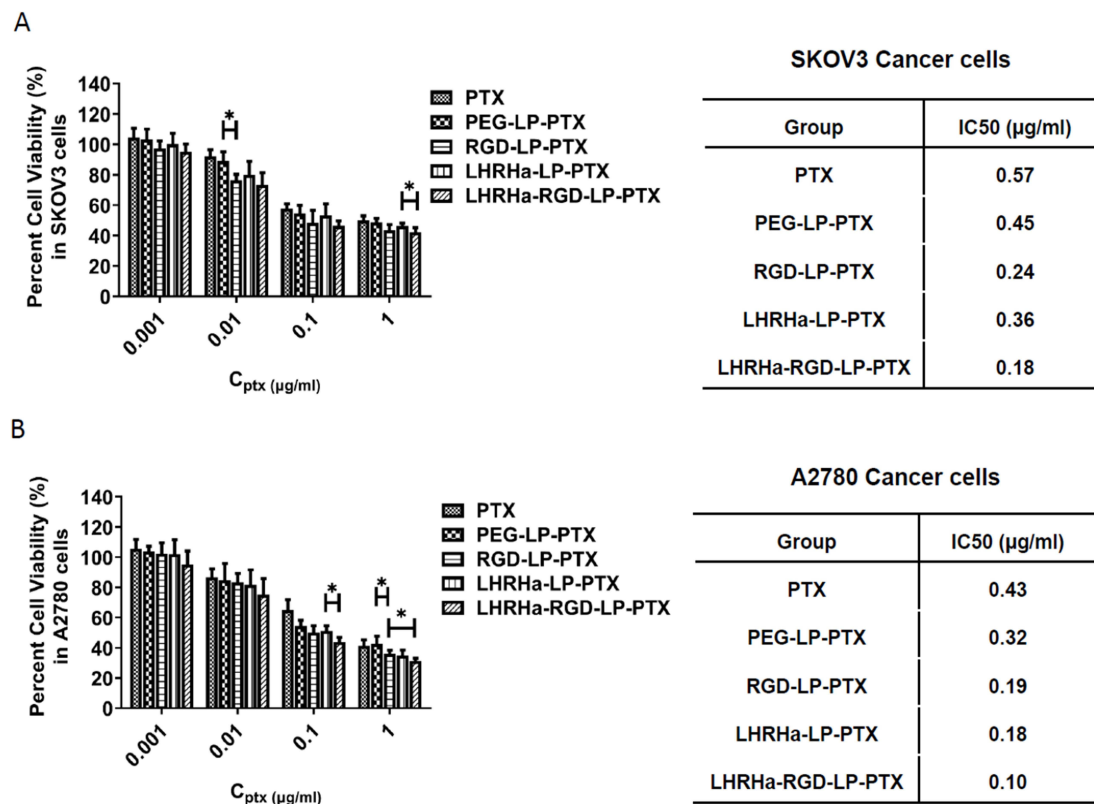
**Figure 2** In vitro Cytotoxicity of PTX and PTX-loaded liposomes. (**A**) Cytotoxicity on SKOV3 cells. (**B**) Cytotoxicity on A2780 cells. Data represented the mean ± SD (n=3). *$p < 0.05$.

cellular uptake in modified liposomes by LHRH receptor or integrin αvβ3 receptor-mediated endocytosis in A2780 cells. Moreover, LHRHa-RGD-LP-PTX showed the highest cytotoxicity on A2780 cells, suggesting a synergistic effect of LHRHa and RGD modifications in enhancing the cytotoxicity of LHRH receptor-positive A2780 cells.

## In vitro Cellular Uptake

LHRH receptor-negative SKOV3 cells and LHRH receptor-positive A2780/DDP cells were used to investigate cellular uptake of modified liposomes. Cellular uptake was evaluated using fluorescence microscopy and a fluorescent microplate reader. The cellular uptake of liposomes in SKOV3 cells is presented in the Figure 3A and B. Compared to the PEG-LP-C6 group, LHRHa modification did not significantly enhance the uptake of LHRHa-LP-PTX in LHRH receptor-negative SKOV3 cells (p > 0.05). However, the cellular uptake of RGD-LP-C6 in SKOV3 cells was significantly higher than that of LHRHa-LP-C6 and PEG-LP-C6 (p < 0.01 for each group). We propose that RGD modification increases the uptake of RGD-LP-C6 in SKOV3 cells through integrin αvβ3 receptor-mediated endocytosis pathways. Additionally, RGD, as a cell-penetrating peptide, can promote modified liposome penetration into tumor cell.[25,26] Therefore, RGD modification plays a critical role in increasing the cellular uptake in SKOV3 cells. Although LHRHa, with a few positive charges, may slightly increase cellular uptake in negatively charged cancer cells through electrostatic interaction,[19] the cellular uptake of LHRHa-RGD-LP-PTX did not significantly enhance compared to RGD-LP-PTX in LHRH receptor-negative SKOV3 cells (p > 0.05).

In Figure 3C and D, the fluorescence intensity of LHRHa-LP-PTX and RGD-LP-C6 groups in A2780/DDP cells was stronger than that of PEG-LP-C6 groups (p < 0.01), and the fluorescence intensity of LHRHa-RGD-LP-C6 groups in A2780/DDP cells was stronger than that of both LHRHa-LP-C6 and RGD-LP-C6 groups (p < 0.01). Our results demonstrate that LHRHa or RGD-conjugated liposomes enhance the uptake of LHRH receptor-overexpressed A2780 cells. Higher cellular uptake could be ascribed to LHRH receptor-mediated endocytosis or integrin αvβ3 receptor-
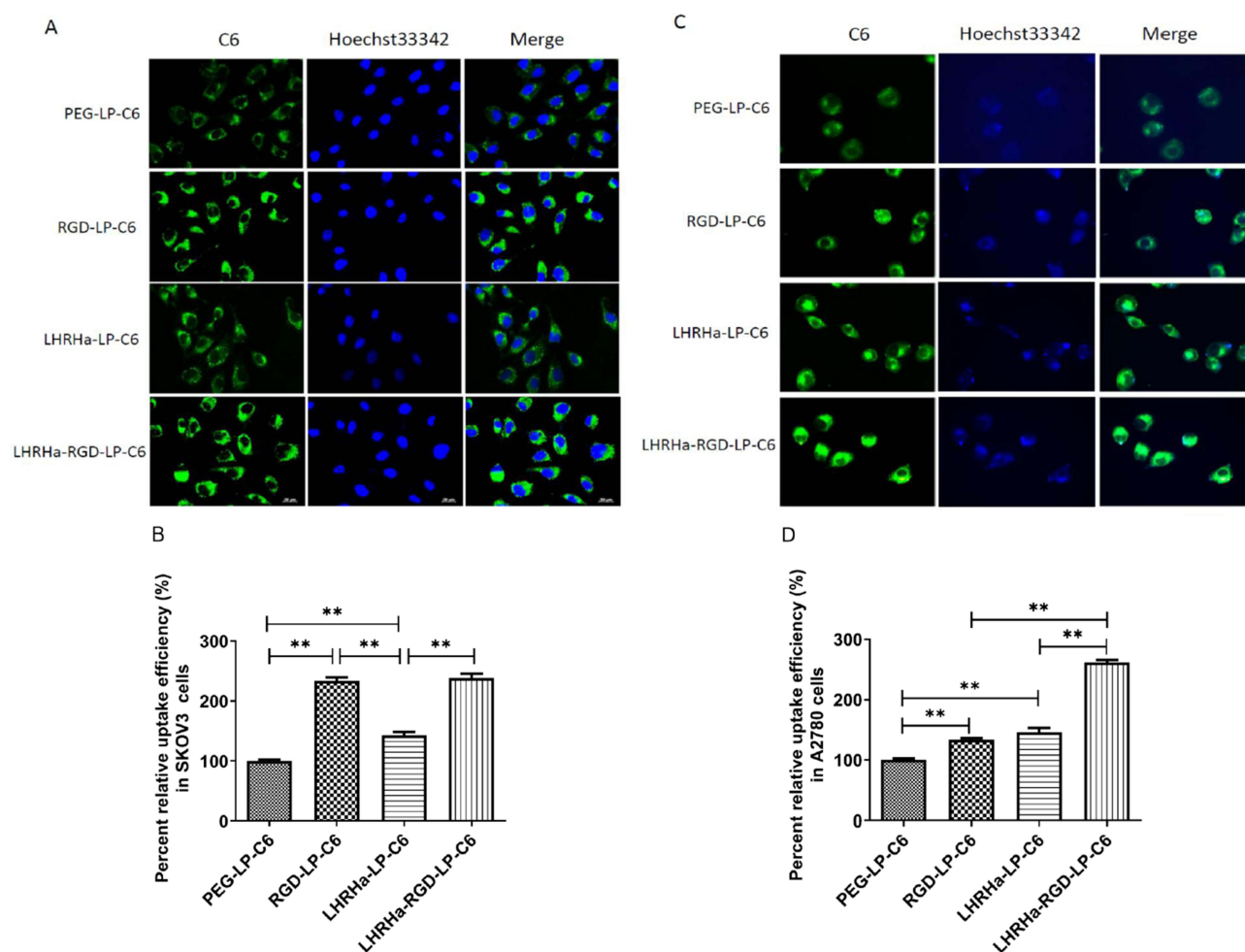
**Figure 3** (**A**) Cellular uptake of C6-loaded liposomes after incubation with SKOV3 cells for 4 h, and Hochest33342 was used for staining nuclei. (**B**) The fluorescence intensity of SKOV3 cells measured using a fluorescent plate reader after being treated with C6-loaded liposomes. **$p< 0.01$. (**C**) Cellular uptake of C6-loaded liposomes after incubation with A2780 cells for 4 h, and Hochest 33342 was used for staining nuclei. (**D**) The fluorescence intensity of A2780 cells measured using a fluorescent plate reader after being treated with C6-loaded liposomes. **$p< 0.01$.

mediated endocytosis.[11,13] Meanwhile, LHRHa and RGD co-modification have a synergistic effect on promoting cellular uptake in LHRH receptor-positive A2780/DDP cells.

## Mechanism of Cellular Uptake

The cellular uptake mechanism of LHRHa-RGD-LP-C6 was further investigated using various endocytic inhibitors. In SKOV3 cells (Figure 4A), compared to the control, the cellular uptake of LHRHa-RGD-LP-C6 decreased by 15.03, 7.32, 28.81, and 26.09% after treatment with filipin, amiloride, cytochalasin D, and chlorpromazine, respectively. The cellular uptake was partially inhibited following treatment with filipin ($p < 0.01$), amiloride ($p >0.05$), cytochalasin D ($p < 0.01$), and chlorpromazine ($p < 0.01$). These results suggest that the cellular uptake of LHRHa-RGD-LP-C6 in SKOV3 cells involves caveolin, actin, and clathrin-mediated endocytosis pathways. In SKOV3 cells, the addition of free LHRHa, in contrast to the control group, did not affect the cellular uptake of LHRHa-RGD-LP-C6 ($p>0.05$), as SKOV3 cells do not express LHRH receptors. However, the addition of free RGD inhibited the cellular uptake of LHRHa-RGD-LP-C6 in SKOV3 cells ($p < 0.01$), and the combined addition of both ligands (RGD and LHRHa) further decreased the uptake ($p<0.01$). This indicates that cellular uptake in SKOV3 cells is primarily through integrin αvβ3 receptor-mediated endocytosis.[13] Free RGD had a significant inhibitory impact on the cellular uptake of LHRHa-RGD-LP-C6 in SKOV3 cells.
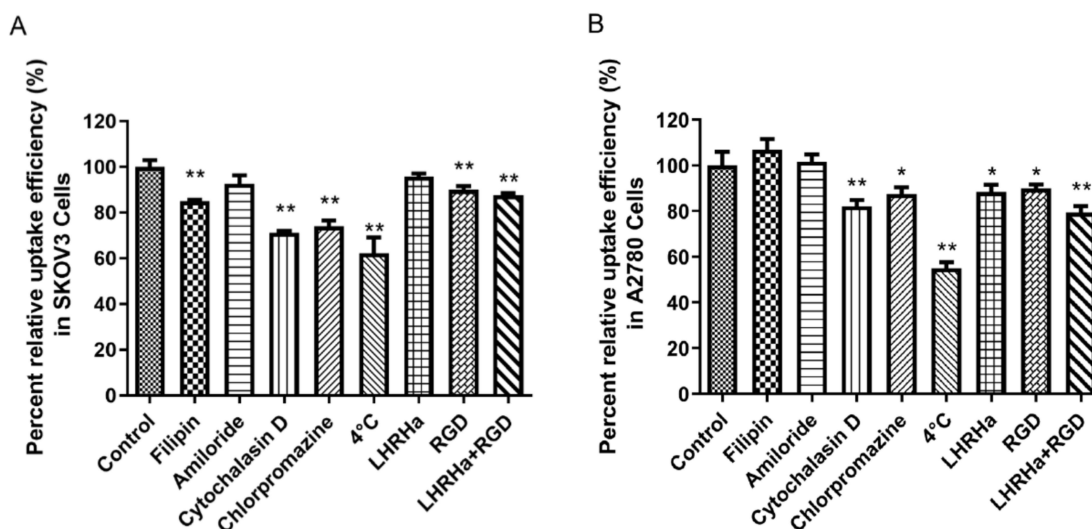
**Figure 4** Uptake mechanism of LHRHa-RGD-LP-C6 after treatment with endocytosis inhibitors. (**A**) SKOV3 cells. (**B**) A2780 cells. Data represented the mean ± SD, n=3, *p< 0.05, **p< 0.01 compared to the non-treated control group.

In contrast, the uptake mechanism of LHRHa-RGD-LP-C6 in A2780 cells (Figure 4B) differed somewhat from that in SKOV3 cells. In A2780 cells, the uptake of LHRHa-RGD-LP-C6 was significantly inhibited by cytochalasin D (p < 0.01) and chlorpromazine (p < 0.05) by 17.85% and 12.55%, respectively, indicating that actin and clathrin-mediated endocytosis are involved in the uptake process. For A2780 cells, the results demonstrated that the addition of free RGD, free LHRHa, and a combination of both competitively inhibited the cellular uptake of LHRHa-RGD-LP-C6. Given the overexpression of both integrin αvβ3 receptor and LHRH receptors on the surface of A2780 cells, we speculate that the uptake of LHRHa-RGD-LP-C6 in A2780/DDP cells involves integrin αvβ3 receptor and LHRH receptor-mediated endocytosis.[11,13] LHRH receptor-mediated endocytosis played a more dominant inhibitory role. Furthermore, in both SKOV3 and A2780 cells, the cellular uptake efficiency of LHRHa-RGD-LP-C6 significantly decreased at 4 °C compared to the control, indicating that energy-dependent endocytosis processes are involved in the uptake of LHRHa-RGD-LP-C6 in these cells.

## In vitro Inhibitory Effect on Tumor Spheroids

Tumor spheroids in vitro more accurately mimic the properties of solid tumors compared to individual tumor cells.[27] To assess the inhibitory effect of modified liposomes on SKOV3 and A2780 tumor spheroids, changes in the spheroids of all groups were monitored under a microscope from Day 0 to Day 8. For SKOV3 tumor spheroids (Figure 5A and B), the longest diameter of spheroids in each group was observed to increase over time. Notably, LHRHa-RGD-LP-PTX exhibited a stronger inhibitory effect on tumor spheroid growth compared to LHRHa-LP-PTX and PEG-LP-PTX (p<0.05). RGD-LP-PTX demonstrated greater tumor spheroid growth inhibition than PTX alone (p<0.05). However, LHRHa-RGD-LP-PTX did not show significantly stronger inhibition than RGD-LP-PTX (p>0.05). These observations align with the results of the in vitro cytotoxicity assays, suggesting that RGD modification plays a major role in enhancing tumor spheroid penetration and cellular uptake in LHRH receptor-negative SKOV3 tumor spheroids.

In the case of A2780 tumor spheroids (Figure 5C and D), on Day 8, the average longest diameter of the tumor spheroids was in the following order: LHRHa-RGD-LP-PTX < LHRHa-LP-PTX < RGD-LP-PTX <PEG-LP-DTX < blank control. Both LHRHa-LP-PTX and RGD-LP-PTX showed a stronger growth inhibitory effect on A2780 tumor spheroids than PEG-LP-DTX and the blank control (p<0.05). Specifically, in the LHRHa-RGD-LP-PTX group, A2780 tumor spheroids became smaller, and there was a noticeable shedding of dead tumor cells. Thus, LHRHa-RGD-LP-PTX had the most pronounced inhibitory effect on the growth of A2780 tumor spheroids, suggesting that these spheroids are more sensitive to RGD and LHRHa co-modified PTX liposomes. This synergistic effect of RGD and LHRHa
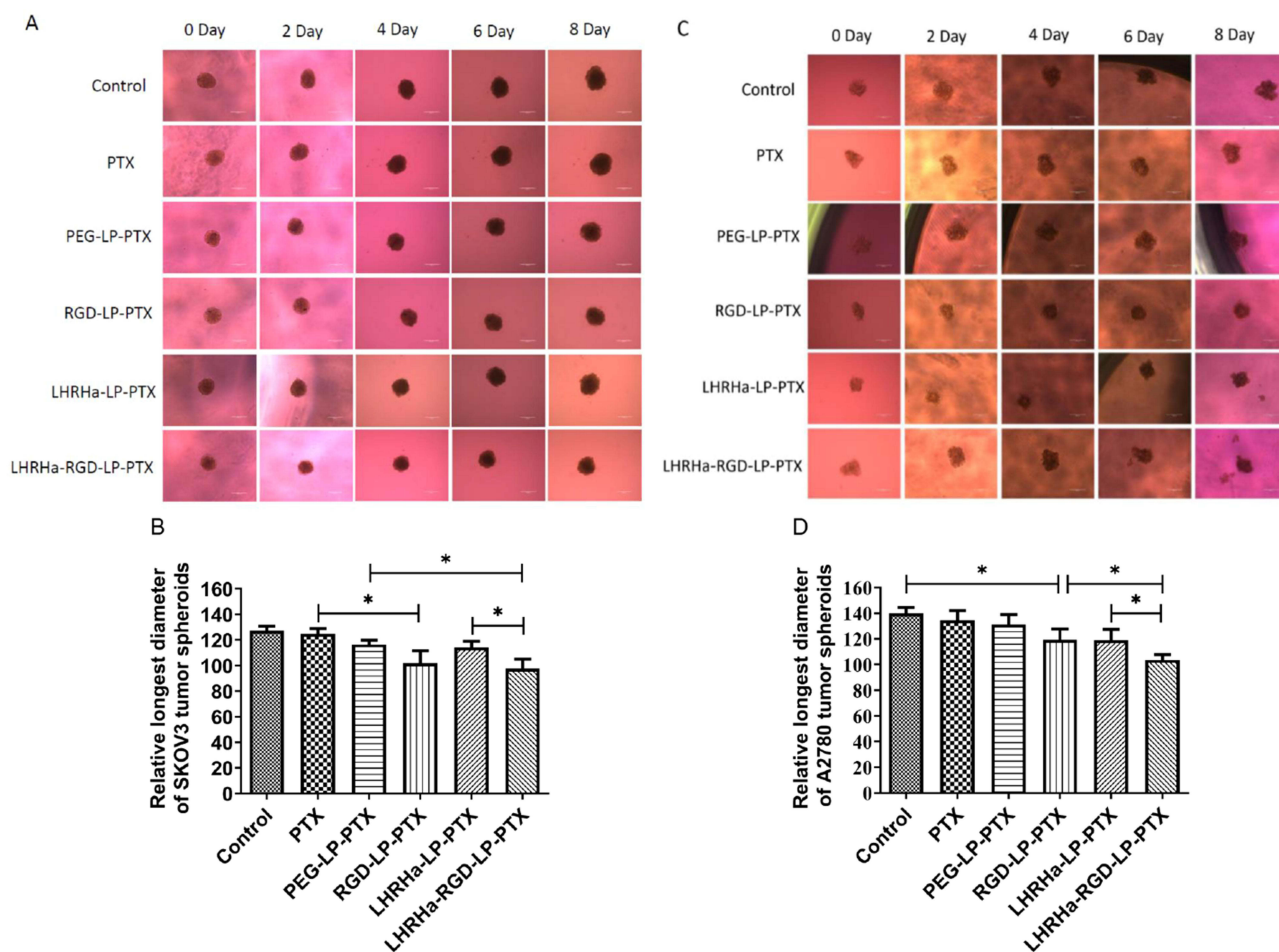
**Figure 5** (**A**) Changes of SKOV3 tumor spheroids treated with PTX formulations. (**B**) Relative longest diameter of SKOV3 tumor spheroids treated with PTX formulations on Day 8 (n=3); *p< 0.05. (**C**) Changes of A2780 tumor spheroids treated with PTX formulations. (**D**) Relative longest diameter of A2780 tumor spheroids treated with PTX formulations on Day 8 (n=3); *p< 0.05. Magnification ×50.

modifications on inhibiting tumor spheroids growth corroborates the in vitro cell viability results obtained using A2780 cells. Based on these findings, we selected the A2780 ovarian tumor-bearing mice model for studying the in vivo anti-tumor efficacy of liposomes.

## Co-Localization of Lysosomes

The confocal microscopy images displaying the co-localization of LHRHa-RGD-LP-C6 within A2780 and SKOV3 cells are depicted in Figure 6A. In both cell types, the majority of green fluorescence (representing LHRHa-RGD-LP-C6) co-localized with the red fluorescence (Lysotracker), resulting in a yellow appearance indicative of endosomes or lysosomes. This suggests that LHRHa-RGD-LP-C6 is predominantly distributed in endosomes or lysosomes following internalization. The scatterplots in Figure 6B, representing red and green intensities, further support this observation. Utilizing Manders' Colocalization Coefficients (MCC) from quantitative confocal analysis,[28,29] a higher degree of co-localization in A2780 cells (MCC=0.86) compared to SKOV3 cells (MCC=0.58) was observed. This indicates a more pronounced co-localization of LHRHa-RGD-LP-C6 within endosomes or lysosome in A2780 cells than in SKOV3 cells. Consequently, upon uptake by ovarian cancer cells, LHRHa-RGD-LP-C6 is internalized via endosomes or lysosome and metabolized through lysosomal pathway.
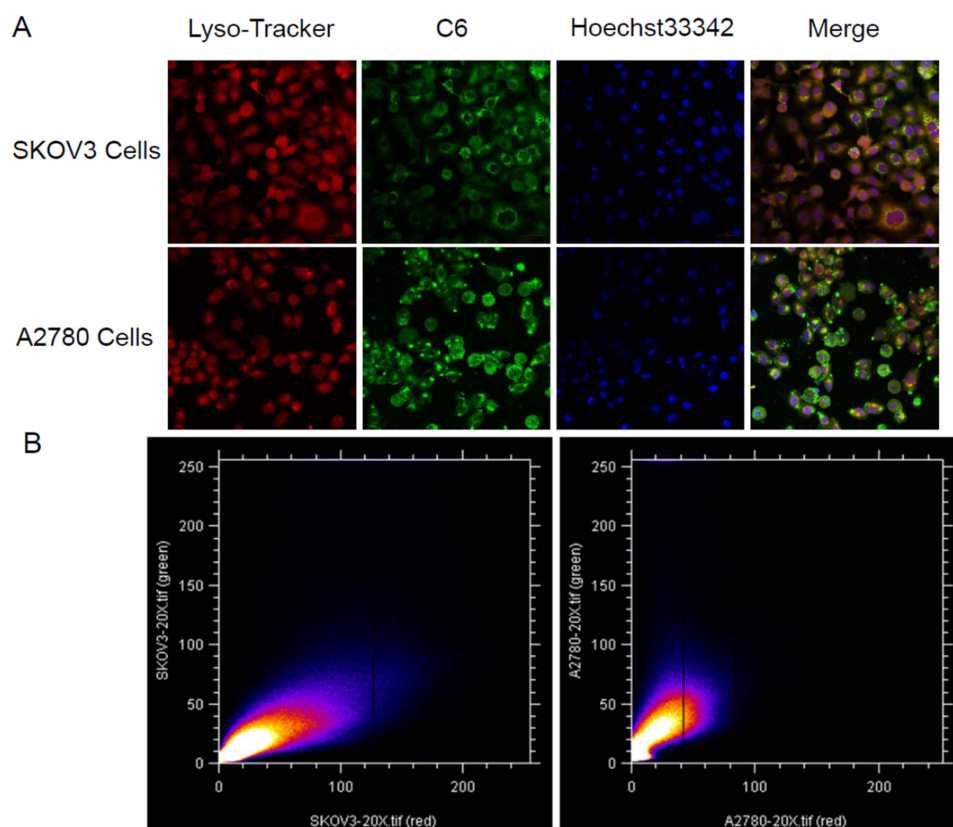
**Figure 6** (**A**) Fluorescence images of SKOV3 and A2780 cells incubated with LHRHa-RGD-LP-C6. Magnification ×200. (**B**) Scatterplot of red and green intensities in the fluorescence images of SKOV3 and A2780 cells.

## In vivo Fluorescent Imaging

The tumor-targeting ability of DiR-labelled liposomes was investigated in subcutaneous A2780 ovarian cancer-bearing BALB/c nude mice through in vivo fluorescent imaging. DiR, a near-infrared fluorescence probe (Ex = 748 nm, Em = 780 nm), was incorporated into the lipid bilayer of the liposomes, allowing DiR fluorescence to reflect the location of the modified liposomes.[30] Real-time in vivo fluorescence imaging of the DiR-loaded liposomes in the mice is shown in Figure 7A. At 4 h post-injection, a high fluorescent signal from the DiR-loaded liposomes was observed throughout the body, indicating widespread distribution. Over time, the fluorescent signal gradually accumulated at the tumor site under the armpit regions. Notably, 24 h after treatment, LHRHa-RGD-LP-DiR displayed a stronger fluorescence intensity at the tumor site compared to other groups. Post-24-hour observation, the mice were euthanized, the important organs and the tumors were collected for ex-vivo imaging (Figure 7B and C). Additionally, the fluorescence intensity at the tumor sites was semi-quantitatively analyzed (Figure 7D). As shown in Figure 7D, LHRHa-LP-DiR and RGD-LP-DiR exhibited higher fluorescence signal accumulation at tumor site than the PEG-LP-DiR group (p<0.01), with LHRHa-RGD-LP-DiR showing the highest signal accumulation (p<0.01). This aligns with the in vitro cellular uptake of LHRHa-RGD-LP-C6 in A2780/DDP cells. The enhanced tumor targeting is attributed to the LHRH receptor and integrin αvβ3 receptor-mediated endocytosis in A2780/DDP cells, which are positive for the LHRH receptor and overexpress the integrin $\alpha v\beta 3$ receptor. LHRHa and RGD co-modification synergistically enhance the tumor-targeting ability in LHRH receptor-positive A2780/DDP cells.

## In vivo Anti-Tumor Efficacy

In this study, we utilized a subcutaneous A2780 ovarian cancer-bearing mice model to evaluate the in vivo anti-tumor efficacy of modified liposomes. Post-treatment with PTX-loaded modified liposomes, the average tumor volume results are depicted in Figure 8A. Both LHRHa-LP-PTX and RGD-LP-PTX groups exhibited a more
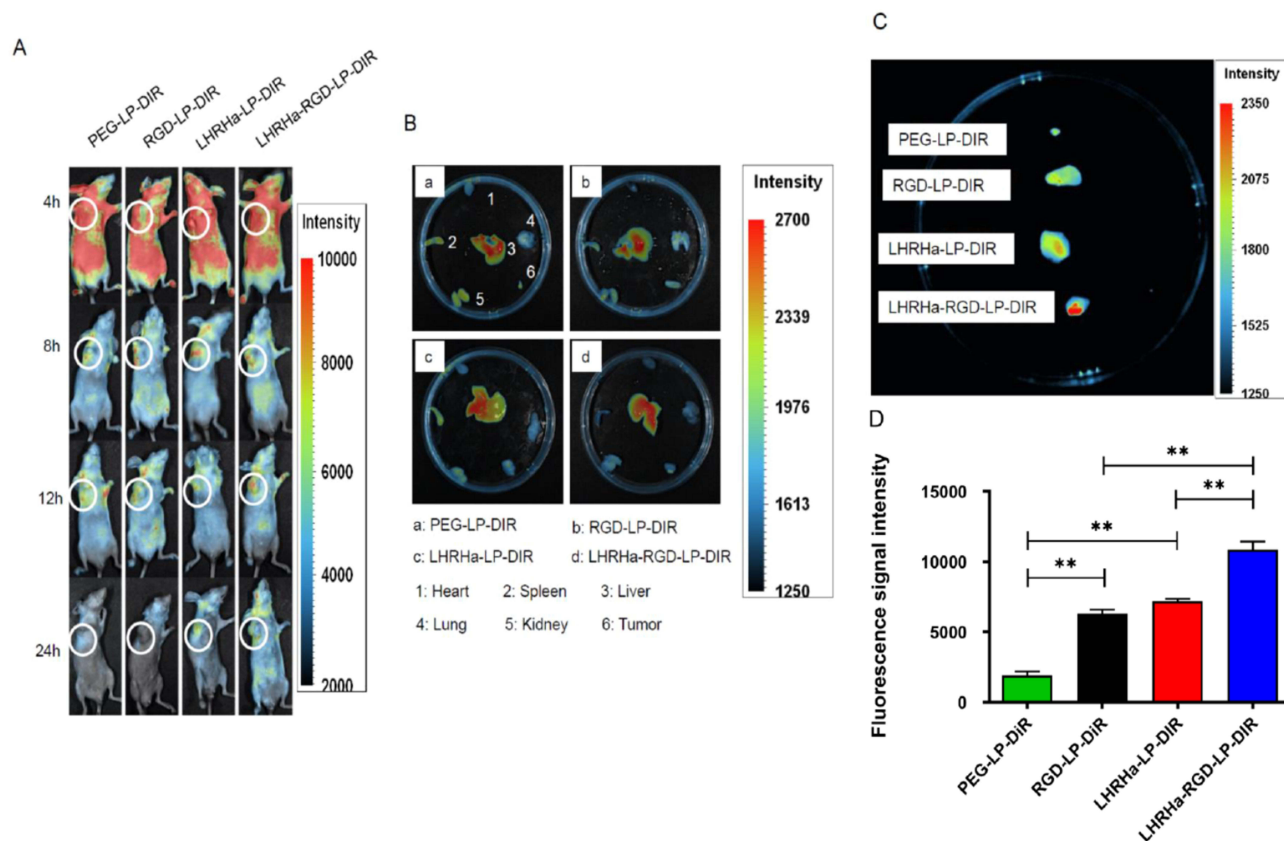
**Figure 7** (**A**) In vivo real-time fluorescence imaging of subcutaneous A2780 ovarian tumor-bearing nude mice treated with DiR-loaded liposomes at 4, 8, 12, and 24 h. (**B**) Fluorescence imaging of important organs collected from different treatment groups. (**C**) Fluorescence imaging of tumors collected from different treatment groups. (**D**) Semi-quantitative fluorescence intensity of ovarian cancer tissues (n=3). **$p < 0.01$.

pronounced growth inhibitory effect on A2780 ovarian cancer compared to the PEG-LP-PTX group ($p<0.05$), indicating an improvement in anti-tumor efficacy with LHRHa or RGD modifications. Notably, LHRHa-RGD-LP-PTX showed the most significant inhibitory effect on tumor growth among all tested groups ($p<0.01$). Figure 8B presents photographs of the excised A2780 ovarian cancer tissues from various treatment groups. As shown in Figure 8C, compared to the tumor weights of LHRHa-LP-PTX (0.76 ± 0. 20 g), RGD-LP-PTX (0.97 ± 0.36 g), PEG-LP-PTX(1.26 ± 0.32 g), and model group (1.90 ± 0.48 g), the tumor weight in the LHRHa-RGD-LP-PTX group (0.29 ± 0.07 g) was significantly lower ($p<0.01$). Furthermore, the anti-ovarian cancer effect in vivo was examined through HE staining and TUNEL fluorescence staining of tumor tissues. HE staining results revealed irregular tumor cells with hyperchromatic nuclei, with the LHRHa-RGD-LP-PTX group showing a reduction in the hyperchromatic area of tumor tissue. TUNEL fluorescence staining results indicates the strongest induction of tumor cell apoptosis in this group, as seem in Figure 8D. The advantage of dual ligand modified delivery system are increasing the cellular uptake, improving accumulation in tumor cells, and enhancing anti-tumor effect. These results corroborate with the in vitro experiment findings, suggesting that LHRHa and RGD co-modified liposomes enhance the in vivo anti-tumor efficacy against LHRH receptor-positive ovarian cancer by increasing tumor tissue apoptosis. This enhanced effect is primarily attributed to increased cellular uptake through LHRH receptor-mediated and integrin αvβ3 receptor-mediated endocytosis. Additionally, RGD, as a cell-penetrating peptide, further facilitates the penetration of LHRHa-RGD-LP-PTX into deeper tumor tissues,[25,26] thereby synergistically enhancing the anti-tumor efficacy.

When LHRHa-RGD-LP-PTX is internalized by tumor cells, it is processed via lysosomal pathways, releasing PTX, which binds to tubulin, promotes microtubule assembly, inhibits depolymerization, arrests the cell cycle at the G2/M phase, and induces apoptosis or necrosis of tumor cells, leading to the anti-tumor effect.[31] Importantly, there was no
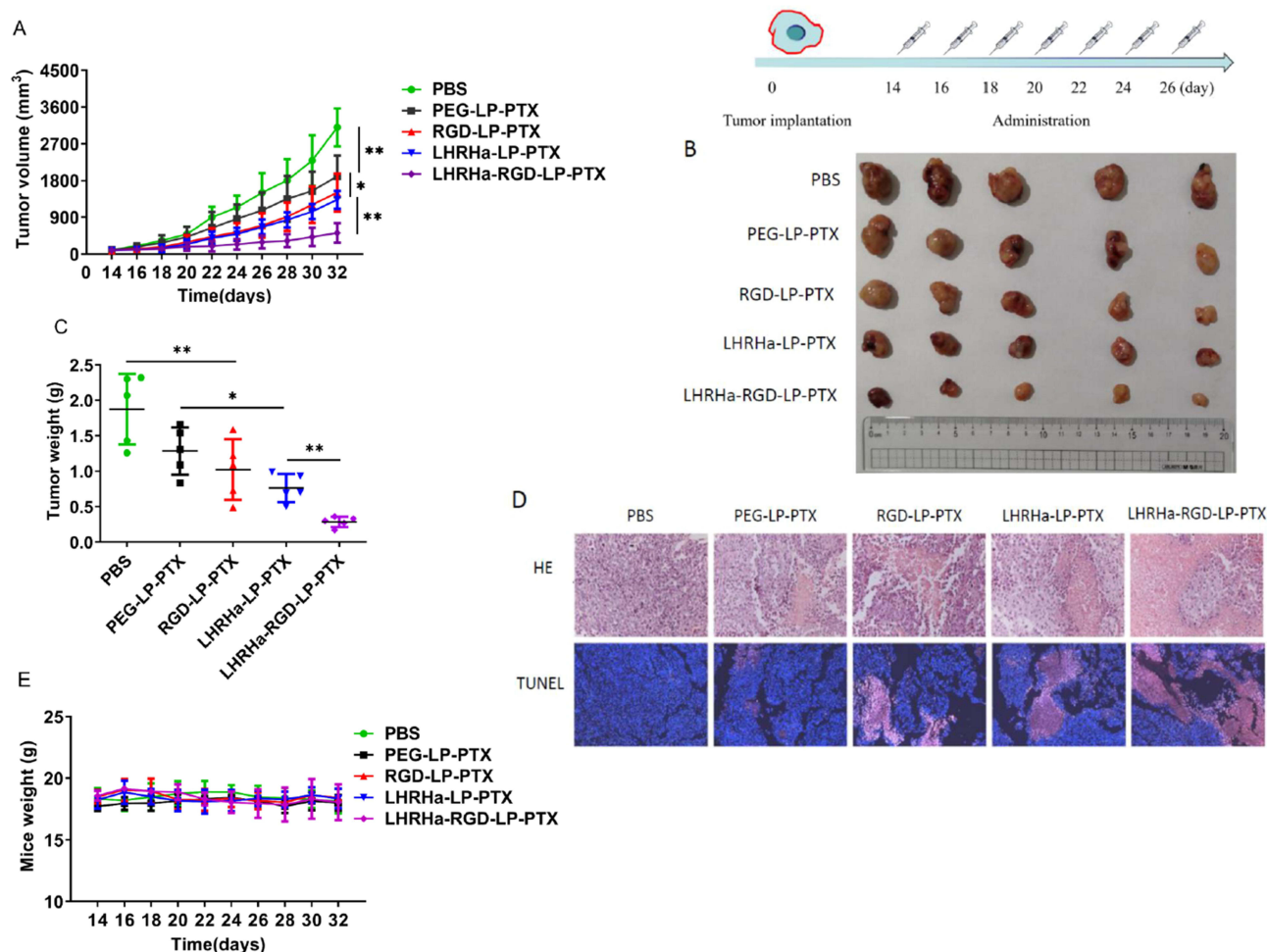
**Figure 8** (**A**) Tumor volume profiles of A2780 tumor-bearing nude mice treated with different formulation groups for 32 days (n=5). *$p < 0.05$, **$p < 0.01$. (**B**) Photographs of excised tumors from A2780 tumor-bearing nude mice treated with various formulation groups. (**C**) Tumor weight of nude mice from all formulation groups (n = 5). *$p < 0.05$, **$p < 0.01$. (**D**) HE and TUNEL fluorescence staining of tumor tissue (HE: magnification ×200; TUNEL: magnification ×100). (**E**) Changes in body weight of A2780 tumor-bearing nude mice (n=5).

significant change in the body weight of ovarian cancer-bearing mice across all groups during the experiment (Figure 8E), indicating the absence of systemic side effects from the formulations. Moreover, HE staining of major organs such as the heart, liver, spleen, lung, and kidney revealed no significant toxicity in any of the formulation groups (Figure S2).

## Conclusions

In this study, we developed LHRHa/RGD co-modified paclitaxel liposomes aimed at enhancing the targeting and therapeutic efficacy against LHRH receptor-positive ovarian cancer. The findings revealed that these co-modified liposomes significantly increased cellular uptake and cytotoxicity in LHRH receptor-positive ovarian cancer cells compared to LHRH receptor-negative cells. Furthermore, LHRHa/RGD co-modified paclitaxel liposomes notably enhanced the in vivo targeting and anti-tumor effects against LHRH receptor-positive ovarian cancer. This enhanced efficacy is likely attributed to mechanisms involving LHRH receptor-mediated and integrin αvβ3 receptor-mediated endocytosis in LHRH receptor-positive ovarian cancer cells. In conclusion, the LHRHa and RGD co-modified paclitaxel liposomes demonstrated synergistic effects in improving tumor targeting and therapeutic outcomes for LHRH receptor-positive ovarian cancers. This strategy holds significant promise for the chemotherapy of LHRH receptor-positive ovarian cancers, offering a targeted approach that could potentially lead to more effective and less toxic treatments.

## Acknowledgments

## Disclosure

The authors declare no conflicts of interest in this work.

## References

1. Chan JK, Kesterson JP, Richardson MT, et al. The clinical and prognostic significance of pre-chemotherapy serum CA-125 in high-risk early stage ovarian cancer: an NRG/GOG ancillary study. *Gynecologic Oncol*. 2022;167(3):429–435. doi:10.1016/j.ygyno.2022.09.028
2. Mailliez A, Pigny P, Bogart E, et al. Is ovarian recovery after chemotherapy in young patients with early breast cancer influenced by controlled ovarian hyperstimulation for fertility preservation or tumor characteristics? Results of a prospective study in 126 patients. *Int J Cancer*. 2022;150 (11):1850–1860. doi:10.1002/ijc.33933
3. Kim SI, Kim JH, Lee S, et al. Hyperthermic intraperitoneal chemotherapy for epithelial ovarian cancer: a meta-analysis. *Gynecol Oncol*. 2022;167 (3):547–556. doi:10.1016/j.ygyno.2022.10.010
4. Huang H, Dong Y, Zhang Y, et al. GSH-sensitive Pt(IV) prodrug-loaded phase-transitional nanoparticles with a hybrid lipid-polymer shell for precise theranostics against ovarian cancer. *Theranostics*. 2019;9(4):1047–1065. doi:10.7150/thno.29820
5. Ye H, Liu X, Sun J, Zhu S, Zhu Y, Chang S. Enhanced therapeutic efficacy of LHRHa-targeted brucea javanica oil liposomes for ovarian cancer. *BMC Cancer*. 2016;16(1):831. doi:10.1186/s12885-016-2870-4
6. Dharap SS, Wang Y, Chandna P, et al. Tumor-specific targeting of an anticancer drug delivery system by LHRH peptide. *Proc Natl Acad Sci USA*. 2005;102(36):12962–12967. doi:10.1073/pnas.0504274102
7. He Y, Zhang L, Song C. PEGylated liposomes modified with LHRH analogs for tumor targeting. *J Control Release*. 2011;152:e29–31. doi:10.1016/ j.jconrel.2011.08.103
8. Linhua Z, Yanqing R, Yong W, Yingna H, Wei F, Cunxian S. Pharmacokinetics, distribution and anti-tumor efficacy of liposomal mitoxantrone modified with a luteinizing hormone-releasing hormone receptor-specific peptide. *Int J Nanomed*. 2018;13:1097–1105. doi:10.2147/IJN.S150512
9. Liu Q, Zhou X, Feng W, Pu T, Xu C. Gonadotropin-releasing hormone receptor-targeted near-infrared fluorescence probe for specific recognition and localization of peritoneal metastases of ovarian cancer. *Front Oncol*. 2020;10:10. doi:10.3389/fonc.2020.00010
10. Sundaram S, Kadam R, Kadam R, Kompella UB. Luteinizing hormone-releasing hormone receptor-targeted deslorelin-docetaxel conjugate enhances efficacy of docetaxel in prostate cancer therapy. *Mol Cancer Ther*. 2009;8(6):1655–1665. doi:10.1158/1535-7163.MCT-08-0988
11. He Y, Zhang L, Song C. Luteinizing hormone-releasing hormone receptor-mediated delivery of mitoxantrone using LHRH analogs modified with PEGylated liposomes. *Int J Nanomed*. 2010;5:697–705. doi:10.2147/ijn.s12129
12. Cheng Y, Ji Y. RGD-modified polymer and liposome nanovehicles: recent research progress for drug delivery in cancer therapeutics - ScienceDirect. *Eur J Pharm Sci*. 2019;128:8–17. doi:10.1016/j.ejps.2018.11.023
13. Song Y, Guo X, Fu J, et al. Dual-targeting nanovesicles enhance specificity to dynamic tumor cells in vitro and in vivo via manipulation of αvβ3-ligand binding. *Acta Pharmaceutica Sinica B*. 2020;11(10):2183–2197. doi:10.1016/j.apsb.2020.07.012
14. Qi N, Zhang S, Zhou X, et al. Combined integrin αvβ3 and lactoferrin receptor targeted docetaxel liposomes enhance the brain targeting effect and anti-glioma effect. *J Nanobiotechnol*. 2021;19(1):446. doi:10.1186/s12951-021-01180-0
15. Faria RS, De lima LI, Bonadio RS, et al. Liposomal paclitaxel induces apoptosis, cell death, inhibition of migration capacity and antitumoral activity in ovarian cancer. *Biomed Pharmacother*. 2021;142:112000. doi:10.1016/j.biopha.2021.112000
16. Tang Z, Feng W, Yang Y, Wang Q. Gemcitabine-loaded RGD modified liposome for ovarian cancer: preparation, characterization and pharma-codynamic studies. *Drug Des Devel Ther*. 2019;13:3281–3290. doi:10.2147/DDDT.S211168
17. Pu C, Chang S, Sun J, Zhu S, Xu RX. Ultrasound-mediated destruction of LHRHa-targeted and paclitaxel-loaded lipid microbubbles for the treatment of intraperitoneal ovarian cancer xenografts. *Mol Pharm*. 2014;11(1):40–48. doi:10.1021/mp400523h
18. Kang S, Duan W, Zhang S, Chen D, Qi N, Qi N. Muscone/RI7217 co-modified upward messenger DTX liposomes enhanced permeability of blood-brain barrier and targeting glioma. *Theranostics*. 2020;10(10):4308–4322. doi:10.7150/thno.41322
19. Qi N, Zhang Y, Tang X, Li A. Cationic/Anionic Polyelectrolyte (PLL/PGA) Coated Vesicular Phospholipid Gels (VPGs) Loaded with Cytarabine for Sustained Release and Anti-glioma Effects. *Drug Des Devel Ther*. 2020;14:1825–1836. doi:10.2147/DDDT.S248362
20. Wei M, Xu Y, Zou Q, et al. Hepatocellular carcinoma targeting effect of PEGylated liposomes modified with lactoferrin. *Eur J Pharm Sci*. 2012;46 (3):131–141. doi:10.1016/j.ejps.2012.02.007
21. Yuan WM, Song QG, Zhang ZR, Fu Y, He Q, He Q. LHRHa aided liposomes targeting to human ovarian cancer cells: preparation and cellular uptake. *Pharmazie*. 2008;63(6):434–438.
22. Hansen CB, Kao GY, Moase EH, Zalipsky S, Allen TM. Attachment of antibodies to sterically stabilized liposomes: evaluation, comparison and optimization of coupling procedures. *BBA*. 1995;1239(2):133–144. doi:10.1016/0005-2736(95)00138-S
23. Kushwah V, Jain DK, Agrawal AK, Jain S. Improved antitumor efficacy and reduced toxicity of docetaxel using anacardic acid functionalized stealth liposomes. Colloids and surfaces. *Biointerfaces*. 2018;172:213–223. doi:10.1016/j.colsurfb.2018.08.047
24. Zou L, Liu X, Li J, Li W, Gu Z. Redox-sensitive carrier-free nanoparticles self-assembled by disulfide-linked paclitaxel-tetramethylpyrazine conjugate for combination cancer chemotherapy. *Theranostics*. 2021;11(9):4171–4186. doi:10.7150/thno.42260
25. Zuo H. iRGD: a promising peptide for cancer imaging and a potential therapeutic agent for various cancers. *J Oncol*. 2019;2019:9367845. doi:10.1155/2019/9367845
26. Guo Z, Li S, Liu Z, Xue W. Tumor-penetrating peptide-functionalized redox-responsive hyperbranched Poly(amido amine) delivering siRNA for lung cancer therapy. *ACS Biomater Sci Eng*. 2018;4(3):988–996. doi:10.1021/acsbiomaterials.7b00971

27. Rui R, Wang H, Yun L. Microfluidic self-assembly of a combinatorial library of single- and dual-ligand liposomes for in vitro and in vivo tumor targeting. *Eur J Pharm Biopharm*. 2018;2(3):243–257.
28. Dunn KW, Kamocka MM, McDonald JH. A practical guide to evaluating colocalization in biological microscopy. *Am J Physiol*. 2011;300(4): C723–742. doi:10.1152/ajpcell.00462.2010
29. Tzaban S, Massol RH, Yen E, et al. The recycling and transcytotic pathways for IgG transport by FcRn are distinct and display an inherent polarity. *J Cell Biol*. 2009;185(4):673–684. doi:10.1083/jcb.200809122
30. Wei L, Guo XY, Yang T, Yu MZ, Chen DW, Wang J-C. Brain tumor-targeted therapy by systemic delivery of siRNA with Transferrin receptor-mediated core-shell nanoparticles. *Int J Pharm*. 2016;510(1):394–405. doi:10.1016/j.ijpharm.2016.06.127
31. Li F, Lu J, Liu J, et al. A water-soluble nucleolin aptamer-paclitaxel conjugate for tumor-specific targeting in ovarian cancer. *Nat Commun*. 2017;8 (1):1390. doi:10.1038/s41467-017-01565-6